Higher order correlation beams in atmosphere under strong turbulence conditions

H. Avetisyan[1,*] **and C. H. Monken**[1]

[1] *Departamento de Física, Universidade Federal de Minas Gerais, Caixa Postal 702, Belo Horizonte, MG 30161-970, Brazil*

[*] *avetisyan@fisica.ufmg.br*

Abstract: Higher order correlation beams, that is, two-photon beams obtained from the process of spontaneous parametric down-conversion pumped by Hermite-Gauss or Laguerre-Gauss beams of any order, can be used to encode information in many modes, opening the possibility of quantum communication with large alphabets. In this paper we calculate, analytically, the fourth-order correlation function for the Hermite-Gauss and Laguerre-Gauss coherent and partially coherent correlation beams propagating through a strong turbulent medium. We show that fourth-order correlation functions for correlation beams have, under certain conditions, expressions similar to those of intensities of classical beams and are degraded by turbulence in a similar way as the classical beams. Our results can be useful in establishing limits for the use of two-photon beams in quantum communications with larger alphabets under atmospheric turbulence.

OCIS codes: (270.0270) Quantum optics; (030.0030) Coherence and statistical optics; (010.1300) Atmospheric propagation.

References and links

1. J. H. Shapiro, "The quantum theory of optical communications," IEEE journal of selected topics in Quantum Electronics **15**, 1547 (2009).
2. Z.-S. Yuan, X.-H. Bao, C-Y. Lu, J. Z., C.-Z. Peng, J.-W. Pan, "Entangled photons and quantum communication," Physics Reports **497**, 140 (2010).
3. A. Mair, A. Vaziri, G. Weihs, and A. Zeilinger, "Entanglement of the orbital angular momentum states of photons," Nature (London) **412**, 313 (2001).
4. D. Bruss, L. Faoro, C. Macchiavello, and G. M. Palma, "Quantum entanglement and classical communication through a depolarising channel," J. Mod. Opt. **47**, 325 (2000).
5. C. King, "The capacity of the quantum depolarizing channel," IEEE Trans. Inform. Theory **49**, 221 (2003).
6. C. Paterson, "Atmospheric turbulence and orbital angular momentum of single photons for optical communication," Phys. Rev. Lett. **94**, 153901 (2005).
7. F. S. Roux, "Infinitesimal-propagation equation for decoherence of an orbital-angular-momentum-entangled biphoton state in atmospheric turbulence," Phys. Rev. A **83**, 053822 (2011); **88**, 049906(E) (2013).
8. D. J. Sanchez and D. W. Oesch, "Orbital angular momentum in optical waves propagating through distributed turbulence," Opt. Express **19**, 24596 (2011).
9. M. Malik, M. O'Sullivan, B. Rodenburg, M. Mirhosseini, J. Leach, M. P. J. Lavery, M. J. Padgett, and R. W. Boyd, "Influence of atmospheric turbulence on optical communications using orbital angular momentum for encoding," Opt. Express **20**, 13195 (2012).
10. F. Tamburini, E. Mari, A. Sponselli, B. Thide, A. Bianchini, and F. Romanato, "Encoding many channels on the same frequency through radio vorticity: first experimental test," New J. Phys. **14**, 033001 (2012).
11. G. Gibson, J. Courtial, M. Padgett, M. Vasnetsov, V. Pas'ko, S. Barnett, and S. Franke-Arnold, "Free-space information transfer using light beams carrying orbital angular momentum," Opt. Express **12**, 5448 (2004).

#248797 Received 28 Aug 2015; revised 1 Oct 2015; accepted 1 Oct 2015; published 29 Jan 2016

12. N. Gisin, G. Ribordy, W. Tittel, and H. Zbinden, "Quantum cryptography," Rev. Mod. Phys. **74**, 145 (2002).
13. B.-J. Pors, C. H. Monken, E. R. Eliel, and J. P. Woerdman, "Transport of orbital-angular-momentum entanglement through a turbulent atmosphere," Opt Express **19**, 6671 (2011).
14. G. Vallone, V. D'Ambrosio, A. Sponselli, S. Slussarenko, L. Marrucci, F. Sciarrino, and P. Villoresi, "Free-space quantum key distribution by rotation-invariant twisted photons," Phys. Rev. Lett. **113**, 060503 (2014).
15. M. Krenn, J. Handsteiner, M. Fink, R. Fickler, A. Zeilinger, "Twisted photon entanglement through turbulent air across Vienna," arXiv:1507.06551.
16. L. C. Andrews and R. L. Phillips, *Laser Beam Propagation Through Random Media* (SPIE, 2005).
17. F. S. Roux, "The Lindblad equation for the decay of entanglement due to atmospheric scintillation," J. Phys. A: Math. Theor. **47**, 195302 (2014).
18. A. L. Moustakas, H. U. Baranger, L. Balents, A. M. Sengupta, S. H. Simon, "Communication through a diffusive medium: coherence and capacity," Science **287**, 287 (2000).
19. S. E. Skipetrov, "Information transfer through disordered media by diffuse waves," Phys. Rev. E **67**, 036621 (2003).
20. D. Elser, T. Bartley, B. Heim, Ch. Wittmann, D. Sych and G Leuchs, "Feasibility of free space quantum key distribution with coherent polarization states," New J. Phys. **11**, 045014 (2009).
21. B. Heim, D. Elser, T. Bartley, M. Sabuncu, C. Wittmann, D. Sych, C. Marquardt, G. Leuchs, "Atmospheric channel characteristics for quantum communication with continuous polarization variables," Appl. Phys. B **98** 635 (2010).
22. A. A. Semenov, F. Toppel, D. Yu. Vasylyev, H. V. Gomonay, and W. Vogel, "Homodyne detection for atmosphere channels," Phys. Rev. A **85**, 013826 (2012).
23. B. Heim, C. Peuntinger, N. Killoran, I. Khan, C. Wittmann, Ch. Marquardt and G. Leuchs, "Atmospheric continuous-variable quantum communication," New J. Phys. **16**, 113018 (2014).
24. M. Mafu, A. Dudley, S. Goyal, D. Giovannini, M. McLaren, M. J. Padgett, T. Konrad, F. Petruccione, N. Lutkenhaus, and A. Forbes, "Higher-dimensional orbital-angular-momentum-based quantum key distribution with mutually unbiased bases," Phys. Rev. A **88**, 032305 (2013).
25. N. D. Leonhard, V. N. Shatokhin, and A. Buchleitner, "Universal entanglement decay in atmospheric turbulence," arXiv:1408.3324.
26. S. E. Skipetrov, "Quantum theory of dynamic multiple light scattering in fluctuating disordered media," Phys. Rev. A **75**, 053808 (2007).
27. S. Smolka, A. Huck, U. L. Andersen, A. Lagendijk, and P. Lodahl, "Observation of spatial quantum correlations induced by multiple scattering of nonclassical light," Phys. Rev. Lett. **102**, 193901 (2009).
28. J. R. Ott, N. A. Mortensen, and P. Lodahl, "Quantum interference and entanglement induced by multiple scattering of light," Phys. Rev. Lett. **105**, 090501 (2010).
29. C. W. J. Beenakker, J. W. F. Venderbos, and M. P. van Exter, "Two-photon speckle as a probe of multi-dimensional entanglement," Phys. Rev. Lett. **102**, 193601 (2009).
30. W. H. Peeters, J. J. D. Moerman, and M. P. van Exter, "Observation of two-photon speckle patterns," Phys. Rev. Lett. **104**, 173601 (2010).
31. H. Di Lorenzo Pires, J. Woudenberg, and M. P. van Exter, "Statistical properties of two-photon speckles," Phys. Rev. A **85**, 033807 (2012).
32. M. Cande and S. E. Skipetrov, "Quantum versus classical effects in two-photon speckle patterns," Phys. Rev. A **87**, 013846 (2013).
33. M. V. da Cunha Pereira, L. A. P. Filpi and C. H. Monken, "Cancellation of atmospheric turbulence effects in entangled two-photon beams," Phys. Rev. A, **88**, 053836 (2013).
34. S. Smolka, J. R. Ott, A. Huck, U. L. Andersen, and P. Lodahl, "Continuous-wave spatial quantum correlations of light induced by multiple scattering," Phys. Rev. A **86**, 033814 (2012).
35. A. K. Jha and R. W. Boyd, "Effects of atmospheric turbulence on the entanglement of spatial two-qubit states," Phys. Rev. A **81**, 053832 (2010).
36. J. Cheng, "Ghost imaging through turbulent atmosphere," Opt. Express **17**, 7916 (2009).
37. C. Li, T. Wang, J. Pu, W. Zhu, R. Rao, "Ghost imaging with partially coherent light radiation through turbulent atmosphere," Appl. Phys. B **99**, 599 (2010).
38. P. Zhang, W. Gong, X. Shen, and S. Han, "Correlated imaging through atmospheric turbulence," Phys. Rev. A **82**, 033817 (2010).
39. K. W. C. Chan, D. S. Simon, A. V. Sergienko, N. D. Hardy, J. H. Shapiro, P. B. Dixon, G. A. Howland, J. C. Howell, J. H. Eberly, M. N. OSullivan, B. Rodenburg, and R. W. Boyd, "Theoretical analysis of quantum ghost imaging through turbulence," Phys. Rev. A **84**, 043807 (2011).
40. S. Smolka, O. L. Muskens, Ad Lagendijk, and P. Lodahl, "Angle-resolved photon-coincidence measurements in a multiple-scattering medium," Phys. Rev. A **83**, 043819 (2011).
41. M. P. van Exter, J. Woudenberg, H. Di Lorenzo Pires, and W. H. Peeters, "Bosonic, fermionic, and anyonic symmetry in two-photon random scattering," Phys. Rev. A **85**, 033823 (2012).
42. M. Mirhosseini, O. S. Magaa-Loaiza, M. N. O'Sullivan, B. Rodenburg, M. Malik, M. P. J. Lavery, M. J. Padget, D. J. Gauthier and R. W. Boyd, "High-dimensional quantum cryptography with twisted light," New J. Phys. **17**,

033033 (2015).
43. S. P. Walborn, C.H. Monken, S. Pádua, P. H. Souto Ribeiro, "Spatial correlations in parametric down-conversion," Phys. Rep. **495**, 87 (2010).
44. G. Gbur and E. Wolf, "Spreading of partially coherent beams in random media," J. Opt. Soc. Am. A **19**, 1592 (2002).
45. T. Shirai, A. Dogariu, and E. Wolf, "Mode analysis of spreading of partially coherent beams propagating through atmospheric turbulence," J. Opt. Soc. Am. A **20**, 1094 (2003).
46. M. Salem, T. Shirai, A. Dogariu, E. Wolf, "Long-distance propagation of partially coherent beams through atmospheric turbulence," Opt. Commun. **216**, 261 (2003).
47. J. C. Owens, "Optical refractive index of air: dependence on pressure, temperature and composition," Appl. Opt. **6**, 51 (1967).
48. V. I. Tatarskii, *Wave Propagation in a Turbulent Medium* (McGraw-Hill, 1961).
49. V. I. Tatarskii, A. Ishimaru, and V. U. Zavorotny, *Wave Propagation in Random Media (Scintillation)*. (SPIE, 1993).
50. M. C. Roggemann and B. Welsh, *Imaging Through Turbulence* (CRC, 1996).
51. R. L. Fante, "Wave propagation in random Media: a system approach," *Progress in Optics*, **22**, 341398 (1985).
52. A. N. Kolmogorov, "The local structure of turbulence in an incompressible viscous fluid for very large Reynolds numbers," C. R. (Doki) Acad. Sci. U.S.S.R. **30**, 301 (1941).
53. V. I. Tatarskii, *The Effects of the Turbulent Atmosphere on Wave Propagation* (transl. for NOAA by Israel Program for Scientific Translations, 1971).
54. T. von Kármán, "Progress in the Statistical Theory of Turbulence," Proceedings of the National Academy of Sciences **34**, 530 (1948).
55. S. M. Rytov, "Diffraction of light by ultrasonic waves," Izvestiya Akademii Nauk SSSR, Seriya Fizicheskaya (Bulletin of the Academy of Sciences of the USSR, Physical Series) **2**, 223259 (1937).
56. A. M. Prokhorov, F. V. Bunkin, K. S. Gochelashvily, and V. I. Shishov, "Laser irradiance propagation in a turbulent media," Proc. IEEE **63**, 790 (1975).
57. A. Ishimaru, *Wave Propagation and Scattering in Random Media* (IEEE, 1997).
58. R. Lutomirski and H. T. Yura, "Propagation of a finite optical beam in an inhomogeneous medium," Appl. Opt. **10**, 1652 (1971).
59. Z. I. Feizulin and Yu. A. Kravtsov, "Expansion of a laser beam in a turbulent medium," Izv. Vyssh., Uchebn. Zaved. Radiofiz. **24**, 1351 (1967).
60. R. Dashen, "Path integrals for waves in random media," J. Math. Phys. **20**, 894 (1979).
61. V. I. Tatarskii and V. U. Zavorotnyi, "Strong fluctuations in light propagation in a randomly inhomogeneous medium," *Progress in Optics III*, E. Wolf, ed. (Elsevier, 1980), pp. 207–256.
62. F. S. Roux, T. Wellens and V. N. Shatokhin, "Entanglement evolution of twisted photons in strong atmospheric turbulence," Phys. Rev. A **92**, 012326 (2015).
63. C. H. Monken, P. H. Souto Ribeiro, and S. Pádua, "Transfer of angular spectrum and image formation in spontaneous parametric down-conversion," Phys. Rev. A. **57**, 3123 (1998).
64. B. E. A. Saleh, M. C. Teich, and A. V. Sergienko, "Wolf equations for two-photon light," Phys. Rev. Lett. **94**, 223601 (2005).
65. L. Mandel and E. Wolf, *Optical Coherence and Quantum Optics* (Cambridge University, 1995).
66. H. van Cittert, "Dié wahrscheinliche schwingungsverteilung in einer von einer lichtquelle direkt oder mittels einer linse beleuchteten ebene," Physica **1**, 201 (1934).
67. F. Zernike, "The concept of degree of coherence and its application to optical problems," Physica **V**, 785 (1938).
68. B. E. A. Saleh, A. F. Abouraddy, A. V. Sergienko, and M. C. Teich, "Duality between partial coherence and partial entanglement," Phys. Rev. A **62**, 043816 (2000).
69. C. Ho, A. Lamas-Linares, C. Kurtsiefer, "Clock synchronization by remote detection of correlated photon pairs," New J. Phys. **11**, 045011 (2009).
70. A. F. Abouraddy, B. E. A. Saleh, A. V. Sergienko, and M. C. Teich, "Role of entanglement in two-photon imaging," Phys. Rev. Lett. **87**, 123602 (2001).
71. N. N. Lebedev, *Special Functions and their Applications* (Prentice-Hall, 1965).
72. A. T. O'Neil, J. Courtial, "Mode transformations in terms of the constituent Hermite-Gaussian or Laguerre-Gaussian modes and the variable-phase mode converter," Opt. Comm. **181**, 35 (2000).
73. C. Y. Young, Y. V. Gilchrest, B. R. Macon, "Turbulence induced beam spreading of higher order mode optical waves," Opt. Eng. **41**, 1097 (2002).
74. I. S. Gradshteyn and I. M. Ryzhik, *Table of Integrals, Series, and Products*, 7th ed. (Academic, 2007).
75. A. Yang, E. Zhang, X. Ji and B. L, "Angular spread of partially coherent Hermite-cosh-Gaussian beams propagating through atmospheric turbulence,"Opt. Express **16**, 8366 (2008).
76. O. Korotkova, L. C. Andrews, and R. L. Phillips, "A model for a partially coherent Gaussian beam in atmospheric turbulence with application in lasercom," Opt. Eng. **43**, 330341 (2004).
77. M. Born and E. Wolf, *Principles of Optics*, 7th ed. (Cambridge University, 1999).

1. Introduction

The study of the effects of turbulent or random media on the propagation of non-classical light has gained a considerable interest due to the possibility of implementing quantum optical communication links with entangled photons [1, 2].

In order to avoid absorption effects in long-distance quantum optical communications, one needs to exploit satellite-based free-space distribution of single photons or entangled photon pairs. In this scheme, photonic quantum states are first sent through the aerosphere, then reflected from one satellite to another, and finally sent back to a ground station. Since the effective thickness of the aerosphere is of the order of $5-10$ km (i.e., the whole aerosphere is equivalent to $5-10$ km ground atmosphere) and photon losses and decoherence are negligible in the outer space, one can achieve global free-space quantum communication as long as the quantum states survive after penetrating the atmosphere.

Transmission through free space can be used as a channel for high-dimensional quantum communication if an orthogonal propagating mode set is used as a d-level system (qudit). In this context, electromagnetic beams carrying orbital angular momentum open an opportunity for communication with large alphabets [3]. Unfortunately, unlike polarization, transverse mode profiles can be severely distorted by turbulence. Transmission through turbulence could thus be regarded as a depolarizing channel for the transverse spatial degrees of freedom [4, 5]. Several theoretical studies have been devoted to the investigation of turbulence effects on the propagation of electromagnetic beams carrying orbital angular momentum [6–9]. An experiment in which orbital angular momentum states in free space propagation were used as a multiplexing resource for classical communication was performed with radio waves (at a wavelength $\lambda = 12.5$ cm) at a 442 m propagation distance [10]. In the optical domain, free-space classical communication using orbital angular momentum has been demonstrated in Ref. [11]. Quantum key distribution through free space should also be considered, since it is possible to distill secure final keys even in the presence of some noise in the quantum channel [12]. The transport of orbital-angular-momentum entanglement through a turbulent atmosphere has been studied experimentally using a turbulence chamber [13]. Alignment-free quantum key distribution through free space for a distance of 210 m exploiting orbital angular momentum in combination with polarization to encode the quantum bits has been demonstrated [14]. A recent experiment demonstrating a distribution of quantum entanglement encoded in orbital angular momentum over a turbulent intra-city link of 3 kilometers has been done [15].

The effects of the atmospheric turbulence can be simulated in the laboratory by artificially inducing random phase fluctuations in optical beams. Most (theoretical and experimental) studies of the effect of atmospheric turbulence on the modal entanglement of photon pairs are based on the single phase screen approach, which uses a single phase screen to model the turbulent atmosphere [16]. The random phase function of such a phase screen represents the phase modulation caused by the turbulence under weak scintillation conditions. An alternative approach valid in all scintillation conditions, the multiple phase screen approach, was recently used to derive first-order differential equations that enable the study of turbulence-induced decoherence of transverse spatial mode entanglement of photon pairs [7, 17]. According to [7], the parameter dependence in the atmospheric decoherence process is more complex than what is found in the single phase screen approach [6].

An appreciable research activity on other related topics has been observed, including: communication [18–23], entanglement in orbital angular momentum [24, 25]; negative correlations [26–28]; two-photon speckle [29–32]; spatial correlations [33–35]; ghost imaging [36–39]; interference, anti-bunching and symmetry properties [40, 41], and high-dimensional quantum cryptography [42].

To the best of our knowledge, no analytical study considering the propagation of *pairs* of

#248797 Received 28 Aug 2015; revised 1 Oct 2015; accepted 1 Oct 2015; published 29 Jan 2016

entangled photons (two-photon beams) through a turbulent atmosphere is available. In this paper we study the optical turbulence effects on a transverse-mode entangled two-photon beam generated by the parametric down-conversion process in a nonlinear $\chi^{(2)}$ crystal [43]. As a result, we calculate the *atmospheric* fourth-order correlation function (the so called two-photon speckle) in the cases when the $\chi^{(2)}$ crystal is pumped by any coherent Hermite/Laguerre-Gauss beam or by a partially coherent beam. In the former case, the higher-order correlation beams can be used for quantum communication tasks with large alphabets if the quantum correlations maintain after propagating through atmosphere. The later case is particularly interesting because the beams produced by partially coherent sources spread less in the random medium than coherent beams [44–46].

The paper is organized as follows: In Sec. 2 we give a brief review of the theory of optical turbulence. In Sec. 3 we develop the study of correlation beams in the atmosphere when the nonlinear crystal is pumped by a coherent beam. In Sec. 4 we extend the theory to the case of partially coherent correlation beams. Finally, in the appendices we provide some derivations of the results discussed in Secs. 3 and 4.

2. Optical Turbulence

In fluid mechanics the Reynolds number is used to help predict similar flow patterns in different fluid/gas flow situations. The Reynolds number is defined as the ratio of momentum forces to viscous forces and quantifies the relative importance of these two types of forces for given flow conditions. A turbulent flow occurs at high Reynolds numbers and is dominated by inertial forces, which tend to produce chaotic eddies, vortices and other flow instabilities. Turbulent air motion represents a set of vortices, or eddies, of various scale sizes, extending from a large scale size L_0 called the *outer scale* of turbulence to a small scale size l_0 called the *inner scale* of turbulence. Under the influence of inertial forces, large eddies break up into smaller ones, forming a continuous cascade of scale sizes between L_0 and l_0 known as the *inertial range*. Scale sizes smaller than the inner scale belong to the *dissipation range*. In the simplest case, when an optical wave propagates through turbulence, the diffraction and scattering effects occur on these eddies of different size (those by molecules or aerosols are neglected). A propagating beam will deflect encountering an eddy that is larger than the beams transverse size, and will expand - encountering an eddy smaller than its size, giving rise to intensity and phase fluctuations, respectively, in the observation plane.

In the *optical turbulence* the most important process in optical wave propagation is the index-of-refraction fluctuations. Fluctuations in the index of refraction are related to temperature and pressure fluctuations. In particular, for optical and infrared wavelengths, the index of refraction for the atmosphere can be written according to [47]

$$n(\mathbf{R}) \simeq 1 + 7.9 \times 10^{-5} \frac{P(\mathbf{R})}{T(\mathbf{R})}, \tag{1}$$

where P is the pressure in millibars, and T is the temperature in Kelvin. There are a number of turbulence models [16, 48–52] depending on whether one includes the effects of the inner or outer scale. The simplest model is the Kolmogorov model for the power spectrum of index-of-refraction fluctuations [52], which is valid in the inertial range between the inner and outer scales:

$$\Phi(\kappa) = 0.033 C_n^2 \kappa^{-11/3}, \qquad 1/L_0 \ll \kappa \ll 1/l_0, \tag{2}$$

where C_n^2 is the index of refraction structure constant (in units of $\mathrm{m}^{-2/3}$). It determines the strength of turbulence, with values ranging from $10^{-17}\mathrm{m}^{-2/3}$ for weak turbulence, to about $10^{-13}\mathrm{m}^{-2/3}$ for strong turbulence.

#248797 Received 28 Aug 2015; revised 1 Oct 2015; accepted 1 Oct 2015; published 29 Jan 2016

To account for the behavior of the power spectrum outside the inertial range, several spectral models were developed. These models include the *Tatarskii spectrum* [53]:

$$\Phi(\kappa) = 0.033 C_n^2 \kappa^{-11/3} \exp\left(-\frac{\kappa^2}{\kappa_m^2}\right), \quad (3)$$

which is valid when $\kappa \gg 1/L_0$; $\kappa_m = 5.92/l_0$, and the (modified) *von Kármán spectrum* [54]:

$$\Phi(\kappa) = 0.033 C_n^2 \kappa^{-11/3} \frac{\exp(-\kappa^2/\kappa_m^2)}{(\kappa^2 + 1/L_0^2)^{11/6}}, \quad (4)$$

valid for $0 \leq \kappa < \infty$; $\kappa_m = 5.92/l_0$. These latter models are not based on rigorous calculations outside the inertial range, but more on mathematical convenience and tractability.

To describe an optical wave propagation through turbulent (random) media several approximation model were developed: the Born approximation, valid under extremely weak turbulence; the Rytov approximation [55], valid under weak turbulence; for strong turbulence, the parabolic equation method [56, 57], extended Huygens-Fresnel principle [58, 59], and the Feynman path integral method [60, 61] have been developed. For non-classical light the parabolic equation method has been used recently [62]. In this paper we adopt the extended Huygens-Fresnel principle.

In the extended Huygens-Fresnel principle, the field that propagates from the source located in the plane $z = 0$ is determined at the point $\mathbf{r} = (x, y)$ of the plane $z = L$ via the expression

$$U(\mathbf{r}, L) = \frac{k e^{ikL}}{2\pi i L} \int\int_{-\infty}^{\infty} d^2 s \, U_0(\mathbf{s}, 0) \exp\left[\frac{ik|\mathbf{s} - \mathbf{r}|^2}{2L} + \psi(\mathbf{r}, \mathbf{s})\right], \quad (5)$$

where $\psi(\mathbf{r}, \mathbf{s})$ is the random part of the complex phase of a spherical wave propagating in the turbulent medium from the point $(\mathbf{s}, 0)$ to the point $(\mathbf{r}, L)$.

If the random medium is statistically homogeneous and isotropic, quantities that take the account of statistical moments of the field are given by [16]

$$E_1(0,0;0,0) \equiv E_1(0) = \langle \psi_2(\mathbf{r}, \mathbf{s}) \rangle + \frac{1}{2} \langle \psi_1^2(\mathbf{r}, \mathbf{s}) \rangle = -2\pi^2 k^2 L \int_0^{\infty} d\kappa \kappa \Phi_n(\kappa), \quad (6)$$

$$E_2(\mathbf{r}_1, \mathbf{r}_2; \mathbf{s}_1, \mathbf{s}_2) = \langle \psi_1(\mathbf{r}_1, \mathbf{s}_1) \psi_1^*(\mathbf{r}_2, \mathbf{s}_2) \rangle = 4\pi^2 k^2 L \int_0^1 d\xi \int_0^{\infty} d\kappa \kappa \Phi_n(\kappa) J_0(\kappa |(1-\xi)\mathbf{p} + \xi \mathbf{Q}|), \quad (7)$$

$$\begin{aligned} E_3(\mathbf{r}_1, \mathbf{r}_2; \mathbf{s}_1, \mathbf{s}_2) &= \langle \psi_1(\mathbf{r}_1, \mathbf{s}_1) \psi_1(\mathbf{r}_2, \mathbf{s}_2) \rangle \\ &= -4\pi^2 k^2 L \int_0^1 d\xi \int_0^{\infty} d\kappa \kappa \Phi_n(\kappa) J_0(\kappa |(1-\xi)\mathbf{p} + \xi \mathbf{Q}|) \exp\left[-\frac{iL\kappa^2}{k} \xi (1-\xi)\right], \end{aligned} \quad (8)$$

where $\xi \equiv 1 - z/L$, and $\mathbf{p} = \mathbf{r}_1 - \mathbf{r}_2$, $\mathbf{Q} = \mathbf{s}_1 - \mathbf{s}_2$.

3. Correlation Beams in the Turbulent Atmosphere

3.1. Correlation Beams

There exist correspondences between the fourth order correlation for the parametric down-conversion field and the second-order correlation for the pump beam. In the degenerate parametric down-conversion process, the two-photon detection probability amplitude (or, equivalently, the fourth-order correlation amplitude) behaves as a Huygens-Fresnel integral for the electromagnetic field of pump propagating from the point $\mathbf{S}$ at $z = 0$ plane to the point $\mathbf{r}$ at the detectors' plane,

$$A(\mathbf{R}_1, \mathbf{R}_2) \propto e^{ik_p z} \int d\mathbf{S} E_p(\mathbf{S}) e^{\frac{ik_p}{2z}(\mathbf{r} - \mathbf{S})^2}. \quad (9)$$

#248797 Received 28 Aug 2015; revised 1 Oct 2015; accepted 1 Oct 2015; published 29 Jan 2016

Here, E_p is the transverse (x,y) profile of the pump beam field, k_p is the wavenumber of the pump beam, $k_s = k_i = k_p/2$, $\mathbf{r} = (\mathbf{r}_1 + \mathbf{r}_2)/2$ and $\mathbf{S} = (\mathbf{s}_1 + \mathbf{s}_2)/2$. In other words,

$$A(\mathbf{R}_1, \mathbf{R}_2) \propto E_p\left(\frac{\mathbf{r}_1 + \mathbf{r}_2}{2}, z\right). \tag{10}$$

Thus we see that the fourth-order correlation amplitude for the field generated by spontaneous parametric down-conversion process resembles a field propagation integral, hence the expression *"correlation beam"*. This effect is a consequence of the transfer of angular spectrum of pump to the downconverted field [63].

3.2. Two Photon Speckle

In order to study the effects of turbulent atmosphere on a non-classical light, e.g. a two-photon field produced by spontaneous parametric downconversion process [43], one needs to take account of the fact that the two-photon (historically called signal and idler) probability amplitude obeys the Wolf equations [64], and therefore exhibits propagation and diffraction phenomena analogous to those of the second-order coherence function, including the Huygens-Fresnel principle and van Cittert-Zernike theorem [65–67]. A duality accompanied with mathematical similarity between the two-photon probability amplitude and the second-order coherence function for the incoherent source has previously been highlighted [68].

In the context of this work, light in a two-photon pure quantum state is described by a superposition of pairs of spatiotemporal single modes, each mode pair with a certain probability of being occupied by just two photons. This state may be entangled in frequencies and in transverse modes.

Assuming that the two-photon state propagates through a random medium and that the coincidence rate P_2 is measured as a function of the positions $\mathbf{R}_1$ and $\mathbf{R}_2$ of the two detectors at times t_1 and t_2, one arrives at the concept of the two-photon speckle pattern $P_2(x_1, x_2)$, where $x_i = (\mathbf{R}_i, t_i)$ [32]. For two independent photons, P_2 factorizes: $P_2(x_1, x_2) = P_1(x_1)P_1(x_2)$, where $P_1(x_i)$ is the probability to detect a photon at a position r_i at a time t_i, $i = 1, 2$. It describes the one-photon speckle pattern and is proportional to the intensity of light at x_i. It is important to realize that P_2 corresponds to a single realization of the random medium. It is therefore a random quantity and fluctuates from one realization of disorder to another. To obtain a deterministic quantity, one must average P_2 over an ensemble of realizations of the random medium. The problem of coincidence identification on the two remote locations without dedicated coincidence hardware is solved using the time correlation of the photon pairs [69].

The two-photon speckle is given by the square magnitude of the two-photon probability amplitude:

$$P_2(x_1, x_2) = |A(x_1, x_2)|^2 = |\langle 0, 0|\hat{E}_2^{(+)}(x_2)\hat{E}_1^{(+)}(x_1)|\psi\rangle|^2, \tag{11}$$

where $x_1 = (\mathbf{r}_1, z_1, t_1)$ and $x_2 = (\mathbf{r}_2, z_2, t_2)$. $\hat{E}_1^{(+)}(x_1)$ and $\hat{E}_2^{(+)}(x_2)$ are $+z$ propagating, scalar, quasi-monochromatic, paraxial, positive-frequency field operators [1] at x_1, x_2. They are expressed in terms of the annihilation operators $\hat{a}_s(x)$ and $\hat{a}_i(x)$ of the signal and idler systems at the source (crystal) plane [68]:

$$\hat{E}_1^{(+)}(x_1) = \int d\mathbf{r}\, h_s(\mathbf{r}_1, \mathbf{r})\hat{a}_s(\mathbf{r}, t_1 - z_1/c), \tag{12}$$

$$\hat{E}_2^{(+)}(x_2) = \int d\mathbf{r}\, h_i(\mathbf{r}_2, \mathbf{r})\hat{a}_i(\mathbf{r}, t_2 - z_2/c), \tag{13}$$

with amplitude-response functions for signal and idler systems:

$$h_j(\mathbf{r}_j, \mathbf{r}) = \frac{k_j e^{ik_j z_j}}{i2\pi z_j} \exp\left\{\frac{ik_j}{2z_j}|\mathbf{r}_j - \mathbf{r}|^2 + \psi^{(j)}(\mathbf{r}_j, \mathbf{r}; k_j)\right\}, \tag{14}$$

#248797 Received 28 Aug 2015; revised 1 Oct 2015; accepted 1 Oct 2015; published 29 Jan 2016

with $j = s, i$. Finally, $|\psi\rangle$ is the two-photon state vector

$$|\psi\rangle = \iint d\mathbf{r}d\mathbf{r}' E_p\left(\frac{\mathbf{r}+\mathbf{r}'}{2}\right)\delta(\mathbf{r}-\mathbf{r}')\hat{a}_s^\dagger(\mathbf{r})\hat{a}_i^\dagger(\mathbf{r}')|0,0\rangle = \int d\mathbf{r} E_p(\mathbf{r})|1_\mathbf{r}, 1_\mathbf{r}\rangle, \tag{15}$$

which is maximally entangled in the configuration space variables. $|1_\mathbf{r}\rangle = \frac{1}{(2\pi)^2}\int d\mathbf{k} e^{i\mathbf{k}\cdot\mathbf{r}}|1_\mathbf{k}\rangle$, $|1_\mathbf{k}\rangle$ being the single photon Fock state of mode $\mathbf{k}$.

Pictorially, the system is presented in the Fig. 1, where, for the completeness, we added an amplitude-response system for the pump as well.

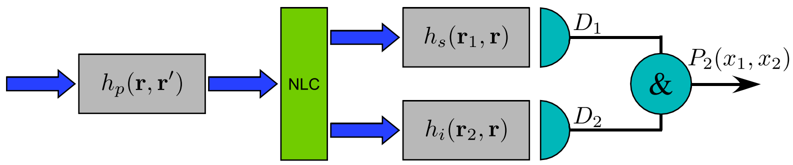

Fig. 1. Schematic diagram of the system considered. NLC represents a nonlinear crystal, h_p, h_s and h_i represent the amplitude response functions for the pump beam (p) and for the down-converted photons (s, i). D_1 and D_2 represent the detectors and P_2 represents the fourth order correlation function, a measurable quantity which is proportional to the two-photon joint detection probability.

When substituting Eqs. (12)-(15) into Eq. (11), the joint detection probability density function takes the following form:

$$P_2(\mathbf{r}_1,\mathbf{r}_2) = \frac{k^2}{4\pi^2 z^2}\iint d\mathbf{r}'d\mathbf{r}'' E_p(\mathbf{r}')E_p^*(\mathbf{r}'')\exp\left\{\frac{ik}{2z}\left[|\mathbf{r}_1-\mathbf{r}'|^2 - |\mathbf{r}_1-\mathbf{r}''|^2 + |\mathbf{r}_2-\mathbf{r}'|^2 - |\mathbf{r}_2-\mathbf{r}''|^2\right]\right\} \times \left\langle \exp\left[\psi(\mathbf{r}',\mathbf{r}_1) + \psi^*(\mathbf{r}'',\mathbf{r}_1) + \psi(\mathbf{r}',\mathbf{r}_2) + \psi^*(\mathbf{r}'',\mathbf{r}_2)\right]\right\rangle, \tag{16}$$

where we dropped the time dependence in field operators and assumed the degenerate case, *i.e.* $k \equiv k_s = k_i = k_p/2$, chose the detection plane at $z \equiv z_1 = z_2$, also took a statistical average over an ensemble of realizations of turbulent medium. Now, with the help of Eqs. (6)-(8) the last exponential in Eq. (16) takes the form

$$\langle \exp[...]\rangle = \exp\left[4E_1(0) + 2E_2(0,0;\mathbf{r}',\mathbf{r}'') + E_2(\mathbf{r}_1,\mathbf{r}_2;\mathbf{r}',\mathbf{r}'') + E_2(\mathbf{r}_2,\mathbf{r}_1;\mathbf{r}',\mathbf{r}'') + 2\mathrm{Re}E_3(\mathbf{r}_1,\mathbf{r}_2;0,0)\right], \tag{17}$$

where it was assumed that the random part of the index-of-refraction is a Gaussian random field, for which $\langle \exp(\psi)\rangle = \exp\left[\langle\psi\rangle + \frac{1}{2}\left(\langle\psi^2\rangle - \langle\psi\rangle^2\right)\right]$ holds. For the case $x_1 = x_2$ the two-photon speckle takes the form

$$P_2(\mathbf{r},\mathbf{r}) = \frac{k^2 e^{-\sigma_{sp}^2(z)}}{4\pi^2 z^2}\iint d\mathbf{r}'d\mathbf{r}'' E_p(\mathbf{r}')E_p^*(\mathbf{r}'')\exp\left\{\frac{ik}{z}\left[|\mathbf{r}-\mathbf{r}'|^2 - |\mathbf{r}-\mathbf{r}''|^2\right] - 2D_{sp}(|\mathbf{r}'-\mathbf{r}''|)\right\}. \tag{18}$$

Experimentally, it can be measured using, e.g., a two-photon absorber [65]. In Eq. (18), $D_{sp}(\rho)$ and $\sigma_{sp}^2(z)$ are the wave structure functions and the scintillation index for a spherical wave, respectively, defined as

$$D_{sp}(Q) = 8\pi^2 k^2 z\int_0^1 d\xi\int_0^\infty d\kappa\kappa\Phi(\kappa)\left[1 - J_0(\kappa\xi Q)\right], \tag{19}$$

and

$$\sigma_{sp}^2(z) = 8\pi^2 k^2 z\int_0^1 d\xi\int_0^\infty d\kappa\kappa\Phi(\kappa)\left[1 - \cos\left(\frac{z\kappa^2}{k}\xi(1-\xi)\right)\right]. \tag{20}$$

#248797 Received 28 Aug 2015; revised 1 Oct 2015; accepted 1 Oct 2015; published 29 Jan 2016

For different models of turbulence power spectrum $\Phi(\kappa)$, they are given in the Appendix III of Ref. [16] expressed in turbulence parameters. Going back to the more general case we recognize in Eq. (17)

$$4E_1(0)+E_2(\mathbf{r}_1,\mathbf{r}_2;\mathbf{r}',\mathbf{r}'')+E_2(\mathbf{r}_2,\mathbf{r}_1;\mathbf{r}',\mathbf{r}'')=-\frac{1}{2}\left[D_{sp}(\mathbf{p},\mathbf{Q})+D_{sp}(-\mathbf{p},\mathbf{Q})\right], \tag{21}$$

and

$$\begin{aligned} 2E_2(0;\mathbf{r}',\mathbf{r}'')+2\mathrm{Re}E_3(\mathbf{r}_1,\mathbf{r}_2;0) &= 8\pi^2k^2z\int_0^1 d\xi\int_0^\infty d\kappa\kappa\Phi(\kappa) \\ &\times\left[J_0(\kappa\xi Q)-J_0(\kappa\xi p)\cos\left(\frac{z\kappa^2}{k}\xi(1-\xi)\right)\right] \\ &= D_{sp}(p)-D_{sp}(Q)+4\pi^2z^3\int_0^1 d\xi\int_0^\infty d\kappa\kappa^5\Phi(\kappa)J_0(\kappa\xi p)\xi^2(1-\xi)^2, \end{aligned} \tag{22}$$

where $D_{sp}(\mathbf{p},\mathbf{Q})$ is the so called two-point spherical wave structure function:

$$D_{sp}(\mathbf{p},\mathbf{Q})=8\pi^2k^2z\int_0^1 d\xi\int_0^\infty d\kappa\kappa\Phi(\kappa)\left[1-J_0(\kappa|(1-\xi)\mathbf{p}+\xi\mathbf{Q}|)\right]. \tag{23}$$

In the last line of Eq. (22), to have an analytical expression, we used geometrical optics approximation, viz. $z\kappa^2/k\ll 1$, to replace $\cos\alpha$ by $1-\alpha^2/2$ ([16], ch.9). Using Tatarskii spectrum (Eq. (3)) we evaluated the integral in Eq. (22) (for details, see the Appendix A). Now Eq. (16) amounts to

$$\begin{aligned} P_2(\mathbf{r}_1,\mathbf{r}_2) &= \frac{k^2}{4\pi^2z^2}\exp\left[\left(\frac{1.58\sigma_{R,p}^2}{\Lambda_{0,p}W_0^2}-\frac{2}{3\rho_{pl}^2}\right)p^2-0.043\pi^2C_n^2z^3p^{-7/3}\right] \\ &\times\iint d\mathbf{S}d\mathbf{Q}E_p(\mathbf{S}+\mathbf{Q}/2)E_p^*(\mathbf{S}-\mathbf{Q}/2)\exp\left[\frac{ik_p}{z}(\mathbf{S}\cdot\mathbf{Q}-\mathbf{r}\cdot\mathbf{Q})\right] \\ &\times\exp\left[-\left(\frac{1.58\sigma_{R,p}^2}{\Lambda_{0,p}W_0^2}+\frac{2}{3\rho_{pl}^2}\right)Q^2\right], \end{aligned} \tag{24}$$

where $\mathbf{r}=(\mathbf{r}_1+\mathbf{r}_2)/2$, $\Lambda_{0,p}=2z/(k_pW_0^2)$, ρ_{pl} is the so called plane-wave spatial coherence radius and $\sigma_{R,p}^2=1.23C_n^2k_p^{7/6}z^{11/6}$ is the Rytov variance.

It is interesting to compare the two photon speckle with the one-photon speckle which is obtained in single photocounts (second order effect). The single-photon probability density is given by [70]

$$P_1(\mathbf{r}_1)=\int d\mathbf{r}|E_p(\mathbf{r})|^2|h_1(\mathbf{r}_1,\mathbf{r})|^2. \tag{25}$$

Substituting the definition (14) in Eq. (25) one arrives at

$$P_1(\mathbf{r}_1)=\left(\frac{k}{2\pi z}\right)^2\int d\mathbf{r}|E_p(\mathbf{r})|^2\exp\left[\psi(\mathbf{r}_1,\mathbf{r};k)+\psi^*(\mathbf{r}_1,\mathbf{r};k)\right]. \tag{26}$$

Expanding ψ, as always, up to the second order, $\psi_1+\psi_2$, $\psi_2\ll\psi_1$, and making an ensemble average of the exponent we obtain

$$\langle\exp\left[\psi(\mathbf{r}_1,\mathbf{r};k)+\psi^*(\mathbf{r}_1,\mathbf{r};k)\right]\rangle=\exp\left[2\sigma_{r_1}^2-T\right], \tag{27}$$

where $\sigma_{r_1}^2$ describes the atmospherically induced change in the mean intensity profile in the transverse direction, and T describes the change in the on-axis mean intensity at the receiver

#248797 Received 28 Aug 2015; revised 1 Oct 2015; accepted 1 Oct 2015; published 29 Jan 2016

plane caused by turbulence [16, Ch. 6]. The one-photon speckle now looks like

$$\begin{aligned} P_1(\mathbf{r}_1) &= \left(\frac{k}{2\pi z}\right)^2 \exp\left[2\sigma_{r_1}^2 - T\right] \int d\mathbf{r} |E_p(\mathbf{r})|^2 \\ &= \left(\frac{k}{2\pi z}\right)^2 \exp\left[2\sigma_{r_1}^2 - T\right] \times I_p|_{z=0}. \end{aligned} \tag{28}$$

It is proportional to the pump intensity at the crystal ($z = 0$), additionally affected by the turbulence parameters represented by $\sigma_{r_1}^2$ and T.

3.3. Coherent Hermite-Gauss and Laguerre-Gauss Pump of any Order.

Now we consider the two-photon speckle for the case when the pump field is a Hermite-Gauss beam

$$E_p(\mathbf{r}) = U_{mn}^{HG}(r_x, r_y, 0) = B_{m,n} H_m\left(\frac{\sqrt{2}}{W_0} r_x\right) H_n\left(\frac{\sqrt{2}}{W_0} r_y\right) \exp\left(-\frac{r^2}{W_0^2}\right), \tag{29}$$

where $H_n(\rho)$ are Hermite polynomials and $B_{m,n} = \left[W_0\sqrt{\pi 2^{m+n+1} m! n!}\right]^{-1}$. In this case Eq. (18) takes the following form

$$\begin{aligned} P_2(\mathbf{r},\mathbf{r}) = \frac{k^2 e^{-\sigma_{sp}^2(z)}}{4\pi^2 z^2} |B_{m,n}|^2 \iint d\mathbf{S} d\mathbf{Q}\, & H_m\left[\frac{\sqrt{2}}{W_0}\left(S_x + \frac{Q_x}{2}\right)\right] H_m\left[\frac{\sqrt{2}}{W_0}\left(S_x - \frac{Q_x}{2}\right)\right] \\ & \times H_n\left[\frac{\sqrt{2}}{W_0}\left(S_y + \frac{Q_y}{2}\right)\right] H_n\left[\frac{\sqrt{2}}{W_0}\left(S_y - \frac{Q_y}{2}\right)\right] \\ & \times \exp\left[-\frac{2}{W_0^2}\left(S_x^2 + S_y^2\right)\right] \exp\left[-\frac{1}{2W_0^2}\left(Q_x^2 + Q_y^2\right)\right] \\ & \times \exp\left[\frac{ik_p}{z}\left(S_x Q_x + S_y Q_y\right)\right] \exp\left[-\frac{ik_p}{z}\left(r_x Q_x + r_y Q_y\right)\right] \\ & \times \exp\left[-\frac{3.16\sigma_{R,p}^2}{\Lambda_{0,p} W_0^2}\left(Q_x^2 + Q_y^2\right)\right], \end{aligned} \tag{30}$$

where we made the following change of variables in the source plane

$$\mathbf{Q} = \mathbf{r}' - \mathbf{r}'', \qquad \mathbf{S} = \frac{1}{2}\left(\mathbf{r}' + \mathbf{r}''\right), \qquad Q = |\mathbf{Q}|, \qquad S = |\mathbf{S}|. \tag{31}$$

In the Appendix B we evaluated this integral analytically. The result is

$$P_2(\mathbf{r},\mathbf{r}) = \frac{e^{-\sigma_{sp}^2(z)}}{2\pi W_{LT}^2} \exp\left[-\frac{2r^2}{W_{LT}^2}\right] \sum_{k=0}^{m}\sum_{l=0}^{n} \binom{m}{k}\binom{n}{l} \left[\frac{W^2}{2W_{LT}^2}\right]^{k+l} \frac{H_{2k}\left[\frac{\sqrt{2}}{W_{LT}} r_x\right] H_{2l}\left[\frac{\sqrt{2}}{W_{LT}} r_y\right]}{k!l!}, \tag{32}$$

where W represents the spot size of the pump beam on the observation plane in the absence of turbulence. We also made the following definition: $W_{LT} \equiv W\sqrt{1 + 6.32\sigma_{R,p}^2 \Lambda}$. Note that, as one would expect, in the no turbulence limit, $\sigma_{sp}^2(z) \to 0, \quad W_{LT} \to W$, and Eq. (32) reduces to

$$P_2(\mathbf{r},\mathbf{r}) = |B_{m,n}|^2 \frac{W_0^2}{W^2} H_m^2\left[\frac{\sqrt{2}}{W} r_x\right] H_n^2\left[\frac{\sqrt{2}}{W} r_y\right] \exp\left[-\frac{2r^2}{W^2}\right], \tag{33}$$

where we have used the identity [71]:

$$H_m^2(x) = 2^m (m!)^2 \sum_{k=0}^{m} \frac{H_{2k}(x)}{2^k (k!)^2 (m-k)!}. \tag{34}$$

Similarly, we have a final expression for $\mathbf{r}_1 \neq \mathbf{r}_2$ case

$$P_2(\mathbf{r}_1,\mathbf{r}_2) = \frac{1}{2\pi W_{LT1}^2} \exp\left[\left(\frac{1.58\sigma_{R,p}^2}{\Lambda_p W^2} - \frac{2}{3\rho_{pl}^2}\right) p^2 - 0.043\pi^2 C_n^2 z^3 p^{-7/3}\right] e^{-\frac{2r^2}{W_{LT1}^2}} \times \sum_{k=0}^{m}\sum_{l=0}^{n} \binom{m}{k}\binom{n}{l}\left[\frac{W^2}{2W_{LT1}^2}\right]^{k+l} \frac{H_{2k}\left[\frac{\sqrt{2}}{W_{LT1}}\left(\frac{r_{x2}+r_{x1}}{2}\right)\right] H_{2l}\left[\frac{\sqrt{2}}{W_{LT1}}\left(\frac{r_{y1}+r_{y2}}{2}\right)\right]}{k!l!}, \tag{35}$$

where $W_{LT1} = W\sqrt{1+6.32\sigma_{R,p}^2\Lambda + \frac{4\Lambda^2 W^2}{3\rho_{pl}^2}}$. Eq. (35) also reduces to an expected expression (see Eq. (10)) for the vacuum limit justifying the concept of the *correlation beam*

$$P_2(\mathbf{r}_1,\mathbf{r}_2) = |B_{m,n}|^2 \frac{W_0^2}{W^2} H_m^2\left[\frac{\sqrt{2}}{W}\left(\frac{r_{x2}+r_{x1}}{2}\right)\right] H_n^2\left[\frac{\sqrt{2}}{W}\left(\frac{r_{y1}+r_{y2}}{2}\right)\right] \exp\left[-\frac{2r^2}{W^2}\right], \tag{36}$$

with $r = |\mathbf{r}_1 + \mathbf{r}_2|/2$.

It is interesting to analyse the $m = 1,\ n = 0$ case, for which Eq. (32) takes the form

$$P_2^{(10)}(\mathbf{r},\mathbf{r}) = \frac{e^{-\sigma_{sp}^2(z)}}{2\pi W_{LT}^2} \exp\left[-\frac{2r^2}{W_{LT}^2}\right]\left(1 + \frac{4W^2}{W_{LT}^4} r_x^2 - \frac{W^2}{W_{LT}^2}\right). \tag{37}$$

In Fig. 2 we plot the normalized version of Eq. (37) as a function of r_x for $r_y = 0$ corresponding to the cases: vacuum, moderate turbulence, moderate-to-strong and strong turbulence for a propagation distance of $z = 5$km. The normalization is made by dividing Eq. (37) by its maximum value $(1/\pi W^2 \mathrm{e})$ in the absence of turbulence. For simplicity, we took $\sigma_{sp}^2(z) = 0.4\sigma_R^2$ for the Kolmogorov spectrum (2) from the Appendix III of ref. [16].

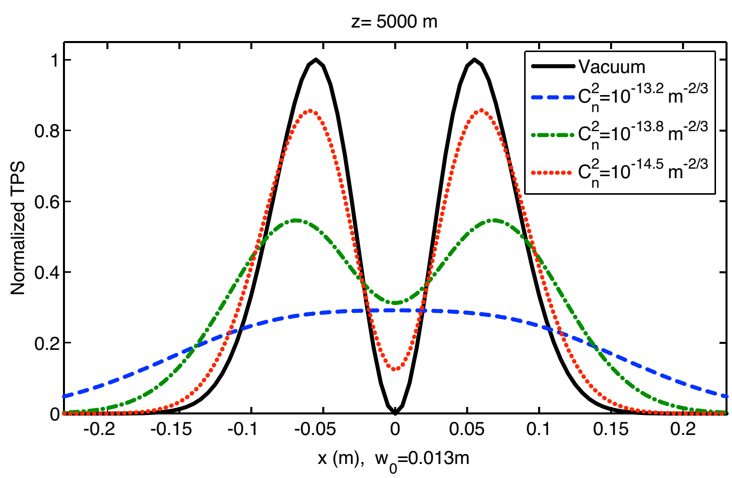

Fig. 2. The normalized two-photon speckle (TPS) for the HG_{10} pump case under turbulence conditions: strong (dashed), strong-to-moderate (dashed-dotted), moderate (dotted) and no turbulence (solid). The normalization is made by dividing Eq. (37) by its maximum value $(1/\pi W^2 \mathrm{e})$ in the absence of turbulence. For simplicity, we took $\sigma_{sp}^2(z) = 0.4\sigma_R^2$ for the Kolmogorov spectrum.

The plot resembles the result [16, ch.17] for HG_{10} laser beam intensity. This is again a manifestation of the beam-like behavior of spatial correlations in two-photon states generated

#248797 Received 28 Aug 2015; revised 1 Oct 2015; accepted 1 Oct 2015; published 29 Jan 2016

by spontaneous parametric down-conversion. We see that the coincident counts reduce significantly in the strong turbulence regime. Another important conclusion can be drawn from this result: the amount of the HG_{00} mode is appreciable even in moderate turbulence, meaning that cross-talk between modes increases with turbulence, degrading the dimensionality of the alphabet based on higher-order Gaussian modes. The dimensionality degradation of Laguerre-Gauss modes due to turbulence has been experimentally demonstrated in Ref. [13].

3.4. Coherent Laguerre-Gauss Pump of any Order.

In calculating the two-photon speckle we have used Hermite-Gauss functions to represent the transverse profile of the pump. We have done so due to relatively simpler manipulations that Hermite-Gauss functions permit, which lacks when dealing with Laguerre-Gauss functions. Using the fact that Hermite-Gauss and Laguerre-Gauss modes are converted one into another by a basis change [72], viz.

$$U_{mn}^{LG}(x,y,z) = \sum_{k=0}^{m+n} i^k b(m,n,k) U_{m+n-k,k}^{HG}(x,y,z), \tag{38}$$

where

$$b(m,n,k) = \sqrt{\frac{(m+n-k)!k!}{2^{m+n}m!n!}} \frac{1}{k!} \frac{d^n}{dt^n} \left[(1-t)^m (1+t)^n\right]_{t=0}, \tag{39}$$

and $m+n = 2p+|l|$, one immediately has a solution for the two-photon speckle for a Laguerre-Gauss pump of any order.

4. Partially Coherent Pump

When the $\chi^{(2)}$ crystal is pumped by a partially coherent beam in the expression for the two-photon speckle (Eq. (16)) one must take the ensemble averaged quantity $\langle E_p E_p^* \rangle$ over different realizations of the field, which, assuming a monochromatic source, is the cross-spectral density function $W^{(c)}(\mathbf{r}_1, \mathbf{r}_2)$, where the superscript (c) indicates the cross-spectral density propagated until the surface of the $\chi^{(2)}$ crystal. The monochromaticity condition is not crucial here since one could use, instead of cross-spectral density function, the mutual coherence function $\Gamma(\mathbf{r}_1, \mathbf{r}_2, \tau)$, which is related with the cross-spectral density function by two-dimensional Fourier transformation. In this case the equation holds for each Fourier component.

The two photon speckle now takes the form

$$\begin{aligned} P_2(\mathbf{r}_1,\mathbf{r}_2) = {} & \frac{k^2}{4\pi^2 z^2} \iint d\mathbf{r}' d\mathbf{r}'' W^{(c)}(\mathbf{r}',\mathbf{r}'') \\ & \times \exp\left\{ \frac{ik}{2z} \left[|\mathbf{r}_1 - \mathbf{r}'|^2 - |\mathbf{r}_1 - \mathbf{r}''|^2 + |\mathbf{r}_2 - \mathbf{r}'|^2 - |\mathbf{r}_2 - \mathbf{r}''|^2 \right] \right\} \\ & \times \exp\left[-\frac{1}{2} \left[D_{sp}(\mathbf{p},\mathbf{Q}) + D_{sp}(-\mathbf{p},\mathbf{Q}) \right] + D_{sp}(p) - D_{sp}(Q) - 0.043\pi^2 C_n^2 z^3 p^{-7/3} \right], \end{aligned} \tag{40}$$

where we dropped the ω-dependence. For the case $x_1 = x_2$ we have

$$\begin{aligned} P_2(\mathbf{r},\mathbf{r}) = {} & \frac{k^2 e^{-\sigma_{sp}^2(z)}}{4\pi^2 z^2} \iint d\mathbf{r}' d\mathbf{r}'' W^{(c)}(\mathbf{r}',\mathbf{r}'') \\ & \times \exp\left\{ \frac{ik}{z} \left[|\mathbf{r} - \mathbf{r}'|^2 - |\mathbf{r} - \mathbf{r}''|^2 \right] - 2D_{sp}(|\mathbf{r}' - \mathbf{r}''|) \right\}. \end{aligned} \tag{41}$$

As a model we choose a Gaussian-Schell-model source, which is characterized by a cross-spectral density function of the form [45,65]

$$W^{(0)}(\mathbf{r}_1,\mathbf{r}_2,\omega) = \sqrt{S^{(0)}(\mathbf{r}_1,\omega) S^{(0)}(\mathbf{r}_2,\omega)} \mu^{(0)}(\mathbf{r}_1,\mathbf{r}_2,\omega), \tag{42}$$

#248797 Received 28 Aug 2015; revised 1 Oct 2015; accepted 1 Oct 2015; published 29 Jan 2016

where

$$S^{(0)}(\mathbf{r},\omega)=M\exp\left[-\frac{|\mathbf{r}|^2}{2\sigma_s^2}\right],\qquad \mu^{(0)}(\mathbf{r}_1,\mathbf{r}_2,\omega)=\exp\left[-\frac{|\mathbf{r}_1-\mathbf{r}_2|^2}{2\sigma_\mu^2}\right] \tag{43}$$

are the spectral density and the spectral degree of coherence of the source, respectively. M is a positive constant, σ_s and σ_μ are the effective widths of spectral density and spectral degree of coherence, respectively. Now one can rewrite Eq. (41) in the form

$$\begin{aligned} P_2(\mathbf{r},\mathbf{r}) &= \frac{k^2 e^{-\sigma_{sp}^2(z)}}{4\pi^2 z^2}\iint d\mathbf{S}d\mathbf{Q}\, W^{(c)}(\mathbf{S}+\mathbf{Q}/2,\mathbf{S}-\mathbf{Q}/2)\exp\left\{\frac{ik_p}{z}\left[\mathbf{S}\cdot\mathbf{Q}-\mathbf{r}\cdot\mathbf{Q}\right]-2D_{sp}(Q)\right\} \\ &= \frac{Mk^2 e^{-\sigma_{sp}^2(z)}}{4\pi^2 z^2}\iint d\mathbf{S}d\mathbf{Q}\,\exp\left[-\frac{S^2}{2\sigma_s^2}-\frac{Q^2}{2\sigma_\Delta^2}\right]\exp\left\{\frac{ik_p}{z}\left[\mathbf{S}\cdot\mathbf{Q}-\mathbf{r}\cdot\mathbf{Q}\right]-2D_{sp}(Q)\right\}, \end{aligned} \tag{44}$$

where $1/\sigma_\Delta^2=1/4\sigma_s^2+1/\sigma_\mu^2$.

The integral (44) evaluates to

$$P_2(\mathbf{r},\mathbf{r})=\frac{Me^{-\sigma_{sp}^2(z)}}{\Delta^2(z)}\exp\left\{-\frac{r^2}{2\sigma_s^2\Delta^2(z)}\right\}, \tag{45}$$

where

$$\Delta^2(z)=1+\frac{1}{(k_p\sigma_s)^2}\left(\frac{1}{4\sigma_s^2}+\frac{1}{\sigma_\mu^2}\right)z^2+\frac{1.58C_n^2k_p^{1/6}}{\sigma_s^2}z^{13/6}. \tag{46}$$

In Eq. (45) $\sqrt{2}\sigma_s\Delta(z)$ represents the overall spread (vacuum and turbulence induced) of the partially coherent two-photon correlation beam. We note that Eq. (45) recovers the result in Ref. [45] for a partially coherent beam but our result is for fourth order correlations. This is a manifestation of the concept of *correlation beam* introduced in Sec. 3.1. Eq. (46) depicts the spread of a partially coherent beam in the atmosphere when the approximation $z\ll z_i$ is satisfied where z_i represents the propagation distance at which the transverse coherence radius of optical wave is of the order of the inner scale l_0. For the other limit, $z\gg z_i$, Eq. (46) takes the following form

$$\Delta^2(z)=1+\frac{1}{(k_p\sigma_s)^2}\left(\frac{1}{4\sigma_s^2}+\frac{1}{\sigma_\mu^2}\right)z^2+\frac{0.55C_n^2l_0^{-1/3}}{\sigma_s^2}z^3. \tag{47}$$

In Eqs. (46) and (47), the first two terms represent the vacuum induced spreading, the third therm – the turbulence induced spreading. As we see from Eqs. (46) and (47), turbulence effects become dominant for long propagation distances. For a fully coherent Gaussian beam ($\sigma_\mu=\infty$), $\Delta^2(z)$ is larger, and (45) is appreciably changed in comparison with the beam propagating in free space. In Fig. 3 we show the normalized version of Eq. (45) for fully and partially coherent Gaussian pump beam cases. The normalization is made by dividing it by the on-axis probability $P_2(\mathbf{r}=0,z)|_{C_n^2=0,\sigma_\mu=0}=M/(1+(\pi z/2k_p\sigma_s^2)^2)$ and by $e^{-\sigma_{sp}^2(z)}$:

$$P_2^N(\mathbf{r},\mathbf{r})=\frac{1+(z/2k_p\sigma_s^2)^2}{\Delta^2(z)}\exp\left\{-\frac{r^2}{2\sigma_s^2\Delta^2(z)}\right\}. \tag{48}$$

As the figures show, the two-photon speckle of the fully coherent correlation beam propagating through the atmospheric turbulence is appreciably changed in comparison with that of the same beam propagating in vacuum, whereas the two-photon speckle of the partially coherent correlation beam is nearly the same as of the correlation beam propagating in vacuum. Thus, in analogy with the classical case [45], partially coherent correlation beams are also less affected by atmospheric turbulence than fully coherent ones. It should be noted that despite this robustness of partially coherent beams to atmospheric turbulence, it is not clear that they can be used to implement larger alphabets for quantum communications.

#248797 Received 28 Aug 2015; revised 1 Oct 2015; accepted 1 Oct 2015; published 29 Jan 2016

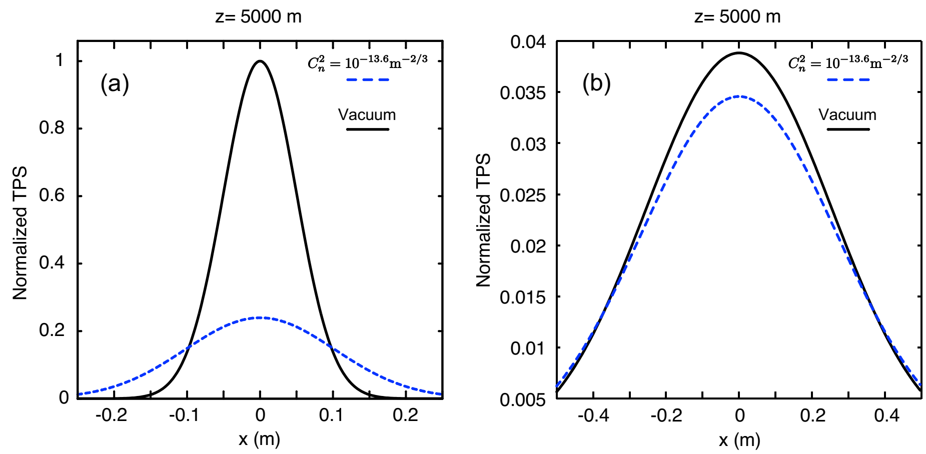

Fig. 3. Normalized two-photon speckle profile for the case when the $\chi^{(2)}$ crystal is pumped by (a) a fully coherent ($\sigma_\mu \to \infty$) Gaussian beam and (b) a partially coherent ($\sigma_\mu = 2$mm) Gaussian beam, both under the conditions $k_p = 10^{-7}\mathrm{m}^{-1}$, $C_n^2 = 10^{-13.6}\mathrm{m}^{-2/3}$, $l_0 = 0.01$m, $\sigma_s = 5$mm.

4.1. Two-Photon Speckle in Coherent-Mode Representation.

The cross-spectral density function of a planar, rectangular Gaussian-Schell-model sources may have coherent-mode representation of the following form [45]

$$W^{(0)}(\mathbf{r}_1, \mathbf{r}_2, \omega) = \sum_m \sum_n \beta_{m,n}(\omega) \phi_n^{(0)*}(\mathbf{r}_1, \omega) \phi_n^{(0)}(\mathbf{r}_2, \omega), \tag{49}$$

where

$$\beta_{m,n}(\omega) = M \left(\frac{\pi}{a+b+c} \right) \left(\frac{b}{a+b+c} \right)^{m+n}, \tag{50}$$

with $a = 1/4\sigma_s^2$, $\quad b = 1/2\sigma_\mu^2$, $\quad c = \sqrt{a^2 + 2ab}$, and the coherent modes $\phi^{(0)}(\mathbf{r}, \omega)$ are given by

$$\phi^{(0)}(\mathbf{r}, \omega) = \phi^{(0)}(r_x, r_y, \omega) = B_{m,n} H_m \left[\frac{\sqrt{2}}{W_0} r_x \right] H_n \left[\frac{\sqrt{2}}{W_0} r_y \right] \exp \left[-\frac{r_x^2 + r_y^2}{W_0^2} \right], \tag{51}$$

with $W_0 = 1/\sqrt{c}$. Using (49) with (51), the two-photon speckle (41) takes the form

$$\begin{aligned} P_2^{(pcoh)}(\mathbf{r}, \mathbf{r}) = & \frac{k^2 e^{-\sigma_{sp}^2(z)}}{4\pi^2 z^2} \sum_m \sum_n \beta_{m,n} |B_{m,n}|^2 \\ & \times \iint d\mathbf{r}' d\mathbf{r}''\, H_m \left[\frac{\sqrt{2}}{W_0} r_x' \right] H_m \left[\frac{\sqrt{2}}{W_0} r_x'' \right] H_n \left[\frac{\sqrt{2}}{W_0} r_y' \right] H_n \left[\frac{\sqrt{2}}{W_0} r_y'' \right] \\ & \times \exp \left[-\frac{r_x'^2 + r_x''^2 + r_y'^2 + r_y''^2}{W_0^2} \right] \exp \left\{ \frac{ik}{z} \left[|\mathbf{r} - \mathbf{r}'|^2 - |\mathbf{r} - \mathbf{r}''|^2 \right] - 2D_{sp}(|\mathbf{r}' - \mathbf{r}''|) \right\}. \end{aligned} \tag{52}$$

We notice that the integral in (52) is exactly the one in (30) if one makes the change of variables (31), so that we can write

$$P_2^{(pcoh)}(x, x) = \sum_{m=0}^{\infty} \sum_{n=0}^{\infty} \beta_{m,n} |B_{m,n}|^2 P_2^{(coh)}(x, x), \tag{53}$$

which is an incoherent sum of probabilities of type (32) with $\beta_{m,n}$ given in (50).

#248797 Received 28 Aug 2015; revised 1 Oct 2015; accepted 1 Oct 2015; published 29 Jan 2016

5. Conclusion

In conclusion, we have analytically derived expressions for joint detection probability density function (two photon speckle) for the correlation beams that propagate through highly turbulent atmosphere. We considered the cases when (i) the beam pumping the $\chi^{(2)}$ crystal in spontaneous parametric down-conversion process is coherent Hermite-Gauss and Laguerre-Gauss beam, and (ii) when it is a partially coherent beam from a Gaussian-Schell model source. The joint detection probability density function for the *partially coherent* source is shown to be an incoherent sum of those for *coherent* sources. In addition, we reproduce, in fourth order correlations, the results in Refs. [16, Ch. 17], [73] and [45], done for classical case *i.e.* in second order correlation for ordinary classical beams.

As a perspective, one can consider the problem for different pump beam models, e.g. cosh-Gauss, Hermite-cosh-Gauss beams [75], Bessel and Bessel-Gauss beams, etc. which have interesting properties and may be applied in communication schemes. As for the partially coherent case one can also consider the *phase screen model* [76] instead of the Gaussian-Schell model we considered here.

An important potential application of our results is the determination of the turbulence parameters: the strength of turbulence σ_R or C_n^2, the inner l_0 and outer L_0 scales, etc. by measuring the signal and idler photons in coincidence. The question whether the correlation beams are advantageous in comparison with a laser beams is still open. The extended Huygens-Fresnel principle that we extensively used for correlation beams can be applied in two-photon imaging systems, together with ABCD ray matrix formalism and Zernike polynomials [77], to calculate the first few turbulence induced aberrations such as piston, tilt, focus, astigmatism, coma and so forth.

Appendix A: Evaluation of the integral in Eq. (22)

$$I = 4\pi^2 z^3 \int_0^1 d\xi \int_0^\infty d\kappa \kappa^5 \Phi(\kappa) J_0(\kappa\xi p)\xi^2(1-\xi)^2. \tag{54}$$

Using Tatarskii spectrum (3), viz.,

$$\Phi(\kappa) = 0.033 C_n^2 \kappa^{-11/3} \exp\left(-\frac{\kappa^2}{\kappa_m^2}\right), \tag{55}$$

we have

$$\int_0^\infty \kappa^{4/3} \exp\left[-\frac{\kappa^2}{\kappa_m^2}\right] J_0(\kappa\xi p) d\kappa = 0.033 C_n^2 \frac{\Gamma(7/6)\kappa^{7/3}}{2} {}_1F_1\left(\frac{7}{6};1;-\frac{\xi^2 p^2 \kappa_m^2}{4}\right), \tag{56}$$

where we used the integral 14 of [16, Appendix II]. ${}_1F_1(a;c;-z)$ is the Confluent Hypergeometric Function.

Now, using the asymptotic form of the Hypergeometric Function for the case $\mathrm{Re}(z) \gg 1$, viz.,

$${}_1F_1(a;c;-z) \sim \frac{\Gamma(c)}{\Gamma(c-a)} z^{-a}, \qquad \mathrm{Re}(z) \gg 1,$$

we can simplify Eq. (56) further:

$$\begin{aligned}\int_0^\infty \kappa^{4/3} \exp\left[-\frac{\kappa^2}{\kappa_m^2}\right] J_0(\kappa\xi p) d\kappa &\approx 0.033 C_n^2 \frac{\Gamma(7/6)}{2\Gamma(1-7/6)} \left(\frac{\xi^2 p^2}{4}\right)^{-7/6} \\ &\approx -0.016 C_n^2 \xi^{-7/3} p^{-7/3}.\end{aligned} \tag{57}$$

This approximation is valid since $\xi^2 p^2 \kappa_m^2/4 \gg 1$ for the following reasons: ξ is a variable that changes between 0 and 1, p is the distance between the detectors, so it can be chosen

#248797 Received 28 Aug 2015; revised 1 Oct 2015; accepted 1 Oct 2015; published 29 Jan 2016

appropriately. Lastly and most importantly, $\kappa_m \equiv 5.29/l_0 \gg 1$ for the inner scale l_0 is a small quantity.

Finally, Eq. (54) takes the form

$$I = -0.046\pi^2 z^3 C_n^2 p^{-7/3} \int_0^1 \xi^{-1/3}(1-\xi)^2 d\xi = -0.043\pi^2 z^3 C_n^2 p^{-7/3}. \tag{58}$$

Appendix B: evaluation of the Integral (30)

$$\begin{aligned} P_2(\mathbf{r},\mathbf{r}) = \frac{k^2 e^{-\sigma_{sp}^2(z)}}{4\pi^2 z^2} \iint d\mathbf{S} d\mathbf{Q}\, & H_m\left[\frac{\sqrt{2}}{W_0}\left(S_x + \frac{Q_x}{2}\right)\right] H_m\left[\frac{\sqrt{2}}{W_0}\left(S_x - \frac{Q_x}{2}\right)\right] \\ & \times H_n\left[\frac{\sqrt{2}}{W_0}\left(S_y + \frac{Q_y}{2}\right)\right] H_n\left[\frac{\sqrt{2}}{W_0}\left(S_y - \frac{Q_y}{2}\right)\right] \\ & \times \exp\left[-\frac{2}{W_0^2}\left(S_x^2 + S_y^2\right)\right] \exp\left[-\frac{1}{2W_0^2}\left(Q_x^2 + Q_y^2\right)\right] \\ & \times \exp\left[\frac{ik_p}{z}\left(S_x Q_x + S_y Q_y\right)\right] \exp\left[-\frac{ik_p}{z}\left(r_x Q_x + r_y Q_y\right)\right] \\ & \times \exp\left[-\frac{3.16\sigma_{R,p}^2}{\Lambda_{0,p} W_0^2}\left(Q_x^2 + Q_y^2\right)\right]. \end{aligned} \tag{59}$$

All the integrals' limits are $\pm\infty$ unless stated otherwise.

Integration in S_x and S_y variables. Separating the S_x integral and calling it I_x we have

$$I_x = \int dS_x\, H_m\left[\frac{\sqrt{2}}{W_0}\left(S_x + \frac{Q_x}{2}\right)\right] H_m\left[\frac{\sqrt{2}}{W_0}\left(S_x - \frac{Q_x}{2}\right)\right] \exp\left[-\left(\frac{2}{W_0^2} S_x^2 - \frac{ik_p Q_x}{z} S_x\right)\right]. \tag{60}$$

The expression in the exponent can be written as

$$\frac{2}{W_0^2} S_x^2 - \frac{ik_p Q_x}{z} S_x = \left(\frac{\sqrt{2}}{W_0} S_x - \frac{ik_p Q_x W_0}{2\sqrt{2}z}\right)^2 + \frac{k_p^2 Q_x^2 W_0^2}{8z^2}.$$

We define $\xi = \frac{\sqrt{2}}{W_0} S_x - \frac{ik_p W_0}{2\sqrt{2}z} Q_x$ so that $dS_x = \frac{W_0}{\sqrt{2}} d\xi$ and

$$\frac{\sqrt{2}}{W_0}\left(S_x \pm \frac{Q_x}{2}\right) = \xi + \frac{Q_x}{\sqrt{2}W_0}\left(i\frac{k_p W_0^2}{2z} \pm 1\right).$$

Now I_x looks like

$$I_x = \frac{W_0}{\sqrt{2}} \exp\left[-\frac{1}{2}\left(\frac{k_p Q_x W_0}{2z}\right)^2\right] \int d\xi H_m[\xi+\eta] H_m[\xi+\zeta] e^{-\xi^2}, \tag{61}$$

where we also defined $\eta = \frac{Q_x}{\sqrt{2}W_0}\left(i\frac{k_p W_0^2}{2z} + 1\right)$ and $\zeta = \frac{Q_x}{\sqrt{2}W_0}\left(i\frac{k_p W_0^2}{2z} - 1\right)$. Using [74, formula 7.377], viz.,

$$\int d\xi\; H_m[\xi+\eta] H_n[\xi+\zeta] e^{-\xi^2} = 2^n \sqrt{\pi} m! \zeta^{n-m} L_m^{n-m}(-2\eta\zeta), \qquad [m \le n],$$

where L_m^α are the generalized Laguerre polynomials, $L_m^0 \equiv L_m$, one arrives at

$$I_x = \frac{W_0}{\sqrt{2}} \exp\left[-\frac{1}{2}\left(\frac{k_p Q_x W_0}{2z}\right)^2\right] 2^m \sqrt{\pi} m! L_m\left[\left(\frac{1}{W_0^2} + \left(\frac{k_p W_0}{2z}\right)^2\right) Q_x^2\right]. \tag{62}$$

#248797 Received 28 Aug 2015; revised 1 Oct 2015; accepted 1 Oct 2015; published 29 Jan 2016

Similar steps bring us to the expression for I_y, viz.,

$$I_y = \frac{W_0}{\sqrt{2}} \exp\left[-\frac{1}{2}\left(\frac{k_p Q_y W_0}{2z}\right)^2\right] 2^n \sqrt{\pi} n! L_n \left[\left(\frac{1}{W_0^2} + \left(\frac{k_p W_0}{2z}\right)^2\right) Q_y^2\right]. \quad (63)$$

Now (59) has the form (note that the coefficients exactly cancel $B_{m,n}^2$)

$$P_2(\mathbf{r},\mathbf{r}) = \frac{k^2 e^{-\sigma_{sp}^2(z)}}{4\pi^2 z^2} \iint dQ_x dQ_y \, L_m(\alpha Q_x^2) L_n(\alpha Q_y^2) \exp[-\beta(Q_x^2+Q_y^2)] \exp\left[-\frac{ik_p}{z}(r_x Q_x + r_y Q_y)\right], \quad (64)$$

where we defined

$$\alpha \equiv \frac{1}{W_0^2} + \left(\frac{k_p W_0}{2z}\right)^2, \qquad \beta \equiv \frac{3.16\sigma_{R,p}^2}{\Lambda_{0,p} W_0^2} + \frac{1}{2W_0^2} + \frac{1}{2}\left(\frac{k_p W_0}{2z}\right)^2 = \frac{3.16\sigma_{R,p}^2}{\Lambda_{0,p} W_0^2} + \frac{\alpha}{2}.$$

Integration in Q_x and Q_y variables. The integral in Q_x, which we call J_x, is the following

$$\begin{aligned} J_x &= \int dQ_x \, L_m[\alpha Q_x^2] \exp\left[-\left(\beta Q_x^2 + \frac{ik_p r_x}{z} Q_x\right)\right] \\ &= \exp\left[-\frac{1}{\beta}\left(\frac{k_p r_x}{2z}\right)^2\right] \int dQ_x \, L_m[\alpha Q_x^2] \exp\left[-\left(\sqrt{\beta} Q_x + \frac{ik_p r_x}{2\sqrt{\beta} z}\right)^2\right]. \end{aligned} \quad (65)$$

Changing the variables $\xi \equiv \sqrt{\beta Q_x}$ and $\eta \equiv -ik_p r_x/(2\sqrt{\beta} z)$, we have

$$J_x = \frac{1}{\sqrt{\beta}} \exp\left[-\frac{1}{\beta}\left(\frac{k_p r_x}{2z}\right)^2\right] \int d\xi L_m\left(\frac{\alpha}{\beta}\xi^2\right) e^{-(\xi-\eta)^2}. \quad (66)$$

Now we use the series representation of the Laguerre polynomial [71]

$$L_m(x) = \sum_{k=0}^{m} \binom{m}{k} \frac{(-1)^k}{k!} x^k,$$

to write the above integral as

$$J_x = \frac{1}{\sqrt{\beta}} \exp\left[-\frac{1}{\beta}\left(\frac{k_p r_x}{2z}\right)^2\right] \sum_{k=0}^{m} \binom{m}{k} \frac{(-1)^k}{k!} \left(\frac{\alpha}{\beta}\right)^k \int d\xi e^{-(\xi-\eta)^2} \xi^{2k}. \quad (67)$$

Using formula $3.462-4$ of Ref. [74],

$$\int dx e^{-(x-y)^2} x^n = (2i)^{-n} \sqrt{\pi} H_n(iy),$$

we arrive at

$$J_x = \frac{1}{\sqrt{\beta}} \exp\left[-\frac{1}{\beta}\left(\frac{k_p r_x}{2z}\right)^2\right] \sum_{k=0}^{m} \binom{m}{k} \frac{(-1)^k}{k!(2i)^{2k}} \left(\frac{\alpha}{\beta}\right)^k H_{2k}\left[\frac{k_p r_x}{2\sqrt{\beta} z}\right]. \quad (68)$$

Integration in Q_y brings us to a similar expression,

$$J_y = \frac{1}{\sqrt{\beta}} \exp\left[-\frac{1}{\beta}\left(\frac{k_p r_x}{2z}\right)^2\right] \sum_{l=0}^{n} \binom{n}{l} \frac{(-1)^l}{l!(2i)^{2l}} \left(\frac{\alpha}{\beta}\right)^l H_{2l}\left[\frac{k_p r_x}{2\sqrt{\beta} z}\right]. \quad (69)$$

#248797 Received 28 Aug 2015; revised 1 Oct 2015; accepted 1 Oct 2015; published 29 Jan 2016

Finally, Eq. (64) takes the following form

$$P_2(\mathbf{r},\mathbf{r}) = \frac{k^2 e^{-\sigma_{sp}^2(z)}}{4\pi z^2 \beta} \exp\left[-\frac{1}{\beta}\left(\frac{k_p r}{2z}\right)^2\right] \sum_{k=0}^{m}\sum_{l=0}^{n} \binom{m}{k}\binom{n}{l} \left[\frac{\alpha^2}{2\beta^2}\right]^{k+l} \frac{H_{2k}\left[\frac{k_p r_x}{2\sqrt{\beta}z}\right] H_{2l}\left[\frac{k_p r_x}{2\sqrt{\beta}z}\right]}{k!l!}. \quad (70)$$

One can write this expression in terms of output pump-beam parameters. To do so, notice that

$$W = W_0\sqrt{1+\Lambda_{0,p}^2} = W_0\Lambda_{0,p}\sqrt{1+\frac{1}{\Lambda_{0,p}^2}} = \frac{2z}{k_p W_0}\sqrt{1+\frac{1}{\Lambda_{0,p}^2}},$$

where we used input parameters $\Theta_0 = 1-\frac{z}{F_0}$, $\Lambda_0 = \frac{2z}{kW_0^2}$ and the output beam parameters $\Theta = 1+\frac{z}{F} = \frac{\Theta_0}{\Theta_0^2+\Lambda_0^2}$, $\Lambda = \frac{2z}{kW^2} = \frac{\Lambda_0}{\Theta_0^2+\Lambda_0^2}$, $\overline{\Theta} = 1-\Theta$, with $\Theta_0 = 1$ for a collimated beam,

$$\alpha = \frac{1}{W_0^2}\left(1+\frac{1}{\Lambda_0^2}\right) = \frac{W^2k_p^2}{4z^2}, \qquad \beta = \frac{3.16\sigma_{R,p}^2}{\Lambda_{0,p}W_0^2} + \frac{\alpha}{2} = \frac{3.16\sigma_{R,p}^2}{\Lambda_p W^2} + \frac{W^2k_p^2}{8z^2},$$

$$\frac{k_p}{2\sqrt{\beta}z} = \frac{k_p}{2z\sqrt{\frac{3.16\sigma_{R,p}^2}{\Lambda_p W^2}+\frac{W^2k_p^2}{8z^2}}} = \frac{\sqrt{2}}{W\sqrt{1+\frac{3.16\sigma_{R,p}^2}{\Lambda_p W^2}\frac{8z^2}{k_p^2W^2}}} \equiv \frac{\sqrt{2}}{W_{LT}},$$

where $W_{LT} \equiv W\sqrt{1+6.32\sigma_{R,p}^2\Lambda}$ and $\beta/\alpha = \left(1+6,32\sigma_{R,p}^2\Lambda\right)/2 = W_{LT}^2/(2W^2)$.

With these formulas, Eq. (70) takes the form

$$P_2(\mathbf{r},\mathbf{r}) = \frac{e^{-\sigma_{sp}^2(z)}}{2\pi W_{LT}^2}\exp\left[-\frac{2r^2}{W_{LT}^2}\right]\sum_{k=0}^{m}\sum_{l=0}^{n}\binom{m}{k}\binom{n}{l}\frac{(W/W_{LT})^{2k+2l}}{2^{k+l}k!l!}H_{2k}\left[\frac{\sqrt{2}}{W_{LT}}r_x\right]H_{2l}\left[\frac{\sqrt{2}}{W_{LT}}r_y\right]. \quad (71)$$

Acknowledgments

The authors acknowledge the financial support from the Brazilian agencies CNPq, CAPES and FAPEMIG.